PROCEEDINGS OF SCIENCE

Study of elemental flux ratios with the ISS-CREAM instrument

Yu Chen,[a,*] Stephane Coutu,[a] Jason T. Link,[b] John W. Mitchell,[c] S. A. Isaac Mognet,[a] Scott L. Nutter,[d] Kenichi Sakai,[c,e] Jacob Smith[f] and Monong Yu[g]

[a]*The Pennsylvania State University, Department of Physics, University Park, PA 16802, USA*
[b]*Laboratory for Atmospheric and Space Physics, University of Colorado, Boulder, CO 80303 USA*
[c]*NASA Goddard Space Flight Center, Astroparticle Physics Laboratory, Greenbelt, MD 20771, USA*
[d]*Northern Kentucky University, Department of Physics, Geology, and Engineering Technology, Highland Heights, KY 41099 USA*
[e]*Center for Research and Exploration in Space Science and Technology (CRESST), UMBC, Baltimore MD, 21250, USA*
[f]*George Mason University, resident at U.S. Naval Research Laboratory, Washington, DC 20375, USA*
[g]*Institut de Física d'Altes Energies (IFAE), 08193 Bellaterra, Barcelona, Spain*

E-mail: yuc357@psu.edu

The origin and propagation of cosmic rays remain open questions in the field of cosmic rays. One way to explore these questions is to study the flux ratios of different elements, including secondary-to-primary ratios. The Cosmic Ray Energetics And Mass instrument on the International Space Station (ISS-CREAM) was built to measure the cosmic-ray elements from protons to iron nuclei with energies up to the cosmic-ray knee. We present the flux ratios of various elements with data collected during ISS-CREAM on-orbit operations, including the boron-to-carbon ratio.

38th International Cosmic Ray Conference (ICRC2023)
26 July - 3 August, 2023
Nagoya, Japan

*Speaker

PoS(ICRC2023)107

1. Introduction

Measurement of elemental fluxes and their ratios is important to uncovering the origin of cosmic rays (CRs). Results from recent experiments have disclosed unexpected features of CR fluxes in greater details than ever before, which have challenged conventional understanding of CRs. For example, it has been shown that the spectra of many elements have a hardening feature around a few hundred GeV/n [1–5]. Although a full explanation is still needed, this structure seems to be associated with the propagation process, which is manifested in the hardening features on the secondary-to-primary ratios [6]. Additionally, it was proposed that primary elements may not share the same origin, especially for protons and He [7], which had been indicated by measurements of their fluxes as well as proton-to-He ratios [8, 9].

The ISS-CREAM instrument is designed to conduct precise measurements of CR fluxes from proton to Fe nuclei in the energy range starting from a few TeV up to the knee and to explore possible features of elemental spectra. In this work, we report on recent progress with the study of elemental flux ratios with the ISS-CREAM data.

2. The ISS-CREAM instrument

2.1 Instrument overview

An expanded view of the ISS-CREAM instrument is shown in Fig. 1. The Silicon Charge Detector (SCD) [10] is a 4-layer detector for charge measurements. The calorimeter (CAL) measures the particle energy through sampling the particle shower - initiated in the C-targets - with its 20 layers of scintillating-fiber ribbons. In addition, the CAL provides a high-energy trigger. The Top and Bottom Counting Detectors (T/BCD) [11] provide a low-energy trigger and the ability to distinguish electrons from protons. The Boronated Scintillator Detector (BSD) [12] measures the tail end of the CAL shower to offer an additional means of identification of electrons and provides an alternative shower energy estimate.

2.2 ISS-CREAM on-orbit operation

The ISS-CREAM instrument was launched on a Falcon rocket from Space-X and deployed on the Japanese Experiment Module - Exposed Facility (JEM-EF) of the ISS on August 22, 2017 and collected data until February 12, 2019. During its operation, it suffered from various types of issues. It was found that only 0.1% of data collected by ISS-CREAM had enough response in the CAL for energy reconstruction, which could be associated with trigger noise, high level of CAL threshold or a combination of both. An alternative on-orbit energy calibration method was proposed to address the possible energy-scale problem with the CAL [13]. In terms of the SCD for charge measurements, its 4^{th} layer was offline most of the time, 3 quadrants of the 3^{rd} layer were on for less than half of the time and 1 quadrant of the 2^{nd} layer was off for about 25% of the time, which makes only the top two layers useful for charge reconstruction.

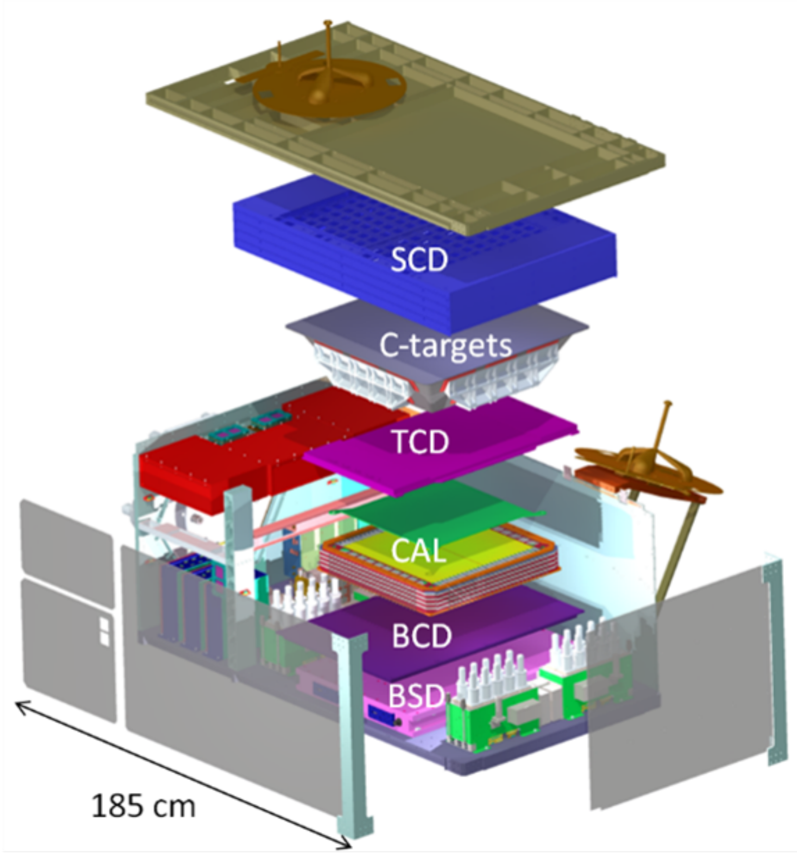

Fig. 1: Expanded view of the ISS-CREAM instrument.

3. Data analysis

3.1 Event selection

Several data selection methods have been used to reduce noise events to a minimal level while still trying to maintain as many low-energy events as possible. A low-energy trigger based on the T/BCD is used in the first step. It is then required that at least 6 consecutive layers in the CAL should each have a minimum of 50 MeV of deposited energy, which is used as a means of a software trigger in place of the CAL trigger which was found to be unreliable or having too high of a threshold. Additionally, a cut based on machine-learning identification of noise patterns [14] is used to remove events that appear have high-energy deposits but do not look like tracks or showers.

Due to possible efficiency issues with the CAL, a pure CAL-based tracking is not functional for lower-energy events. Therefore, a tracking method that combines information from the TCD, 2 layers of the SCD and the CAL is adopted. A so-called 'seed method' searches for the highest activities on the TCD where the top few pixels with the highest signals are considered as possible seeds and the seed with the highest signal sum including its neighboring pixels gets selected as the hit. This helps discriminate an isolated pixel that outshines all other channels due to noise or an extraneous off-track particle depositing all its energy in this pixel. The hits in the TCD and the top 2 layers of the SCD are used to define a raw track before signals of the CAL around the track are used to further improve the directional reconstruction. Fig. 2 shows the performance of the multi-layer tracking method compared to one type of CAL-based tracking method in terms of tracking efficiency in the top two layers of the SCD. The efficiencies are calculated with simulated events that consist of all elements (from p to Fe nuclei) of cosmic rays with a power-law energy distribution. Additionally, for the best tracking results, the final selected events are required to have reconstructed tracks going through all layers of the CAL and the SCD and the intersection of the track with the TCD and the BCD should agree with their signal-weighted center as well.

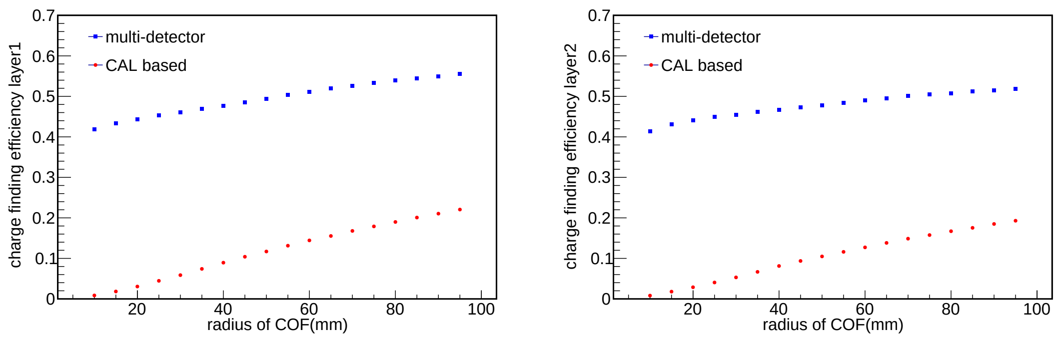

Fig. 2: Performance of the multi-layer tracking method compared to one type of CAL-based tracking method in terms of tracking efficiencies in the top layer (left) and the second layer (right) of the SCD. The tracking efficiency is defined as the frequency when the correct charge pixel appears within the circumference of a circle of confusion (COF) centered on the extrapolated point of the tracking method on a given layer of the SCD.

Lastly, a charge consistency cut is applied which requires that the charge measurements from the first 2 layers of the SCD should both be non-zero and agree within 1 charge unit. The charge of the particle in an event is taken as the mean of the two charge measurements. This requirement further reduces possible noise events due to noise pixels on the SCD and improves the charge resolution. On the other hand, the requirement of two layers effectively reduces the sensitive area of the instrument to 3/4 since 1/4 of layer 2 of the SCD is dead most of the time.

3.2 Background estimate

The selected events are used to fill a charge histogram that covers the range from p to Fe. A multi-charge-peak fit is then attempted where p and He are assumed to have Landau distributions and other elements considered (B, C, O, Fe etc.) are assumed to follow Gaussian distributions. Fig. 3 shows one example of such fits. For a given element of interest with a nominal charge Z_0, suppose function $f_1(Z)$ describes its charge distribution as a function of a measured charge Z, and $f_2(Z)$ describes the sum of charge distributions of all other elements ($Z \neq Z_0$), the true number of count of this element is defined as

$$N \times \frac{\int_{\max(0,Z_0-5)}^{Z_0+5} f_1 \mathrm{d}Z}{\int_{\max(0,Z_0-0.5)}^{Z_0+0.5} (f_1 + f_2) \mathrm{d}Z} \tag{1}$$

where N is the count of that element in a normal search window ($Z_0 - 0.5$, $Z_0 + 0.5$). This formula also tries to account for the possible overflow of the element outside the search window with a

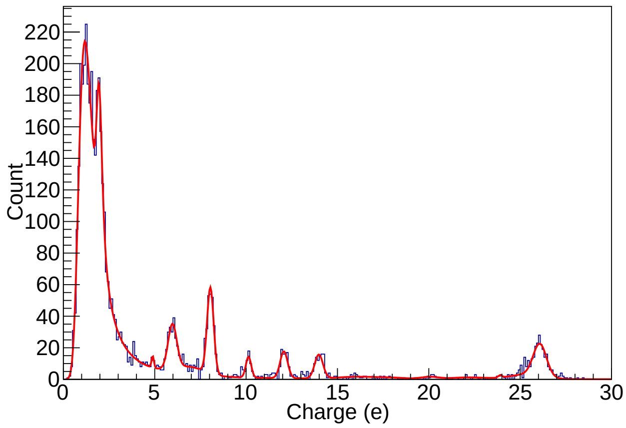

Fig. 3: Charge distribution with ISS-CREAM data used for background estimate. The p and He populations are not well disambiguated in this study and are not used here directly.

bigger integration interval of $(Z_0 - 5, Z_0 + 5)$ which is sufficient since one expects the usual charge width of ~ 0.2 charge units. On the other hand

$$1 - \frac{\int_{\max(0, Z_0 - 5)}^{Z_0 + 5} f_1 \mathrm{d}Z}{\int_{\max(0, Z_0 - 0.5)}^{Z_0 + 0.5} (f_1 + f_2) \mathrm{d}Z} \tag{2}$$

characterizes the amount of background contamination for a specific element.

As the spectra of secondary species fall faster than the primary with energy, one expects the background contamination to be larger with higher energy for elements like B. Therefore, it is ideal to conduct the background estimate in a similar manner for different energies, as will be illustrated in more details in the next section.

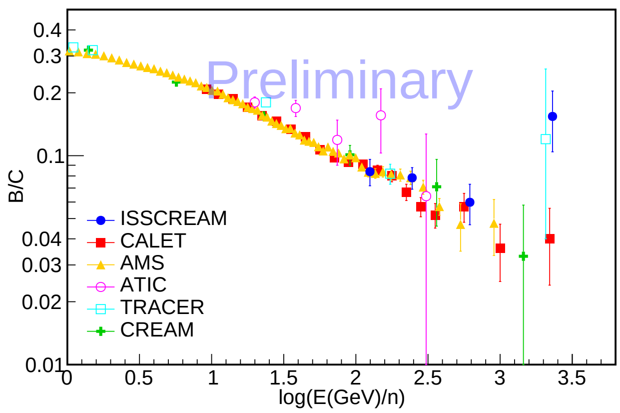

Fig. 4: Boron-to-carbon ratio with the ISS-CREAM data. The reference points are collected from [15–19].

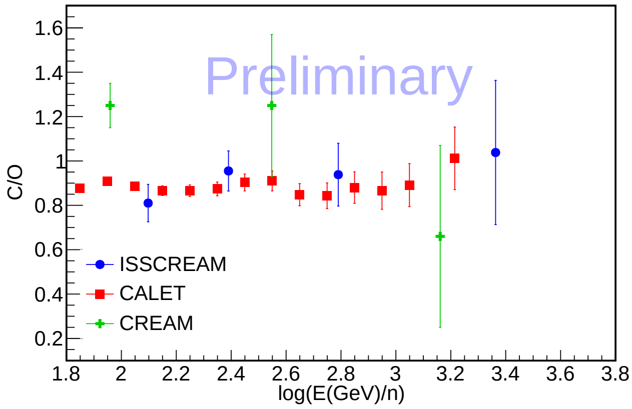

Fig. 5: Carbon-to-oxygen ratio with the ISS-CREAM data. The reference points are collected from [19, 20].

3.3 Results

A simple linear conversion method in energy reconstruction is adopted using Geant4 simulation of the ISS-CREAM instrument that maps out the relation of dE/dx in the CAL with the true kinetic energy of the particles. The reconstructed energy is further divided into 4 energy bins in kinetic energy per nucleon. On the other hand, the background estimate is performed in the bins of kinetic energy (by converting these bins into total kinetic energy using carbon's mass number as an approximation). This is because contamination comes from other elements with roughly the same kinetic energy regardless of their true charge and mass number. In addition, it's worth noting that the current background estimate is not perfect with a few caveats limited by the ISS-CREAM data: 1. The highest energy bin has limited statistics therefore the same background estimate determined when combing data events from the highest two bins is applied to the highest two bins separately in determining the ratios. 2. The true energy threshold of the instrument is unknown and a conservative lower bound is picked for the lowest bin, which also results in uncertainties in its background estimate. Currently, the background for this bin is estimated with a charge histogram that is filled with all events that pass the selection cuts with just a higher-energy bound of this bin but without a lower-energy requirement.

The count of each element for each energy bin is corrected with the background and the elemental ratios are calculated by dividing the background-corrected count of one element by the other. This procedure assumes equal selection efficiency for the elements of interest. The B-to-C ratio and C-to-O ratio with ISS-CREAM data in this study are shown in Figs. 4 and 5, respectively. The error bars are statistical only while assuming the background estimate is precise and causes no additional uncertainties. Further investigation into possible systematic uncertainties is underway.

Acknowledgments

This work was supported in the U.S. by NASA grants NNX17AB43G, NNX17AB42G, and their predecessor grants, as well as by directed RTOP funds to NASA GSFC. The authors also thank M. Geske, Penn State, for contributions to the BSD, and K. Wallace at Northern Kentucky

University for contributions to Monte Carlo simulations. We also recognize the contributions of past CREAM and ISS-CREAM collaborators.

References

[1] H. S. Ahn, P. Allison, M. G. Bagliesi, J. J. Beatty, G. Bigongiari, J. T. Childers et al., *Discrepant hardening observed in cosmic-ray elemental spectra*, *The Astrophysical Journal* **714** (2010) L89.

[2] O. Adriani, G. C. Barbarino, G. A. Bazilevskaya, R. Bellotti, M. Boezio, E. A. Bogomolov et al., *PAMELA measurements of cosmic-ray proton and helium spectra*, *Science* **332** (2011) 69.

[3] M. A. Aguilar, O. Demakov, Y. Lu, U. Becker, N. Attig, T. Li et al., *Observation of the identical rigidity dependence of He, C, and O cosmic rays at high rigidities by the Alpha Magnetic Spectrometer on the International Space Station*, *Physical Review Letters* **119** (2017) .

[4] M. Aguilar, L. Ali Cavasonza, G. Ambrosi, L. Arruda, N. Attig, F. Barao et al., *Properties of neon, magnesium, and silicon primary cosmic rays results from the Alpha Magnetic Spectrometer*, *Physical Review Letters* **124** (2020) .

[5] M. Aguilar, L. A. Cavasonza, M. Allen, B. Alpat, G. Ambrosi, L. Arruda et al., *Properties of iron primary cosmic rays: Results from the Alpha Magnetic Spectrometer*, *Physical Review Letters* **126** (2021) .

[6] M. Aguilar, L. Ali Cavasonza, G. Ambrosi, L. Arruda, N. Attig, S. Aupetit et al., *Observation of new properties of secondary cosmic rays lithium, beryllium, and boron by the Alpha Magnetic Spectrometer on the International Space Station*, *Physical Review Letters* **120** (2018) .

[7] C. Evoli, R. Aloisio and P. Blasi, *Galactic cosmic rays after the AMS-02 observations*, *Physical Review D* **99** (2019) 103023.

[8] M. Aguilar, D. Aisa, B. Alpat, A. Alvino, G. Ambrosi, K. Andeen et al., *Precision measurement of the proton flux in primary cosmic rays from rigidity 1 GV to 1.8 TV with the Alpha Magnetic Spectrometer on the International Space Station*, *Physical Review Letters* **114** (2015) 171103.

[9] M. Aguilar, D. Aisa, B. Alpat, A. Alvino, G. Ambrosi, K. Andeen et al., *Precision measurement of the helium flux in primary cosmic rays of rigidities 1.9 GV to 3 TV with the Alpha Magnetic Spectrometer on the international space station*, *Physical Review Letters* **115** (2015) 211101.

[10] J. Lee, Y. Amare, T. J. Anderson, D. Angelaszek, N. B. Anthony, K. Cheryian et al., *The ISS-CREAM silicon charge detector for identification of the charge of cosmic rays up to Z = 26: Design, fabrication and ground-test performance*, *Astroparticle Physics* **112** (2019) 8.

[11] Y.-S. Hwang, H.-C. Kim, T. J. Anderson, D. Angelaszek, M. Copley, S. Coutu et al., *Construction and testing of a top counting detector and a bottom counting detector for the Cosmic Ray Energetics And Mass experiment on the international space station*, *Journal of Instrumentation* **10** (2015) P07018.

[12] Y. Amare, T. J. Anderson, D. Angelaszek, N. Anthony, K. Cheryian, J.-Y. Choi et al., *The boronated scintillator detector of the ISS-CREAM experiment*, *Nuclear Inst. and Methods in Physics Research, A* **943** (2019) 162413.

[13] Y. Chen, T. Anderson, S. Coutu, T. LaBree, J. Link, J. W. Mitchell et al., *On-orbit energy calibration of the calorimeter on the ISS-CREAM instrument using the boronated scintillator detector*, *Proceedings of the 37th International Cosmic Ray Conference (Berlin, Germany)* **395** (2022) 074.

[14] M. Yu, T. Anderson, Y. Chen, S. Coutu, T. LaBree, J. Link et al., *Machine learning applications on event reconstruction and identification for ISS-CREAM*, *Proceedings of the 37th International Cosmic Ray Conference (Berlin, Germany)* **395** (2022) 061.

[15] AMS Collaboration, M. Aguilar, L. Ali Cavasonza, G. Ambrosi, L. Arruda, N. Attig et al., *Precision Measurement of the Boron to Carbon Flux Ratio in Cosmic Rays from 1.9 GV to 2.6 TV with the Alpha Magnetic Spectrometer on the International Space Station*, *Physical Review Letters* **117** (2016) 231102.

[16] CALET Collaboration, O. Adriani, Y. Akaike, K. Asano, Y. Asaoka, E. Berti et al., *Cosmic-Ray Boron Flux Measured from 8.4 GeV/n to 3.8 TeV/n with the Calorimetric Electron Telescope on the International Space Station*, *Physical Review Letters* **129** (2022) 251103.

[17] A. D. Panov, N. V. Sokolskaya, J. Adams, J. H., H. S. Ahn, G. L. Bashindzhagyan, K. E. Batkov et al., *Relative abundances of cosmic ray nuclei B-C-N-O in the energy region from 10 GeV/n to 300 GeV/n. results from ATIC-2 (the science flight of ATIC)*, *Proceedings of the 30th International Cosmic Ray Conference (Merida, Mexico)* (2008) 3–6.

[18] A. Obermeier, M. Ave, P. Boyle, C. Höppner, J. Hörandel and D. Müller, *Energy spectra of primary and secondary cosmic-ray nuclei measured with tracer*, *The Astrophysical Journal* **742** (2011) 14.

[19] H. Ahn, P. Allison, M. Bagliesi, J. Beatty, G. Bigongiari, P. Boyle et al., *Measurements of cosmic-ray secondary nuclei at high energies with the first flight of the CREAM balloon-borne experiment*, *Astroparticle Physics* **30** (2008) 133.

[20] O. Adriani and others, *Direct Measurement of the Cosmic-Ray Carbon and Oxygen Spectra from 10 GeV/n to 2.2 TeV/n with the Calorimetric Electron Telescope on the International Space Station*, *Physical Review Letters* **125** (2020) 251102.